Proceedings of the Czech–Japanese Seminar in Applied Mathematics 2006
Czech Technical University in Prague, September 14-17, 2006
pp. 72–80

A CONVENIENT WORKING ASSUMPTION FOR THE DEVELOPMENT OF NUMERICAL MODELS OF HIGH-PRESSURE INDUCTIVELY COUPLED PLASMA FLOWS

RADEK HONZÁTKO[1] , DAVID VANDEN-ABEELE[2] , ANDREA LANI[2] , MARCO PANESI[2] , TIAGO QUINTINO[2] , AND HERMAN DECONINCK[2]

Abstract.
We present preliminary numerical simulations of inductively coupled plasma flows in an existing plasma tunnel of the von Karman Institute. Emphasis is put on the numerical techniques used to create the model. As a useful working assumption, we propose to neglect the plasma-induced electro-magnetic field in a first implementation. While this approximation is shown to be inaccurate, it is nevertheless very useful since it allows to obtain physically consistent preliminary results with a minimal effort.

Key words. Inductively coupled plasma, local thermodynamic equilibrium, finite-volume method, Navier-Stokes equations.

AMS subject classifications. 74A15, 76D05, 76X05, 80A32

1. Introduction. The high-pressure Inductively Coupled Plasma (ICP) torch is a plasma source which allows to generate thermal plasmas with peak temperatures $\sim 10\,000$ K in a clean, electrodeless manner. A gas is injected in a swirling, annular way into a heat-resistant quartz tube, surrounded by an inductor (see Figure 1.1). A radio-frequency electric current runs through the inductor and induces a secondary current through the gas inside the tube, which heats up by means of Ohmic dissipation. The swirling injection of gas close to the quartz wall stabilizes the plasma by promoting flow recirculation [7]. Because of their chemical purity and good stability, high-pressure ICPs are well-suited for a variety of industrial and scientific applications [3]. Note that the ICPs studied here operate at pressures greater than 1000 Pa and are not to be confused with the inductive discharges at very low pressures used, e.g., for the processing of semi-conductors.

Over the past three decades, considerable efforts have been invested in the development of reliable numerical simulations of high-pressure ICPs; the pioneering work in the field is due to Boulos ([2], 1976). In the authors' option, the most challenging part in the development of numerical models of ICPs is that both a flow and electromagnetic field solver must be run in a coupled manner. In this contribution, we investigated the usefulness of a pragmatic working assumption, in which the electromagnetic field induced by an ICP is completely neglected in the preliminary model development. Under this simplifying assumption, preliminary ICP results may be obtained by merely including two source terms into an existing low-Mach number Navier-Stokes solver. These source terms represent the action of the external electromagnetic field, induced by the coil surrounding the ICP torch. We will assess the

[1]Department of Technical Mathematics, Faculty of Mechanical Engineering, Czech Technical University in Prague, Prague, Czech Republic.
[2]Aeronautics and Aerospace Department, von Karman Institute for Fluid Dynamics, Rhode Saint Genése, Belgium.

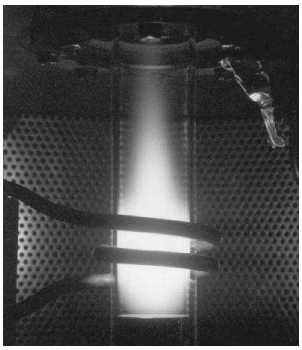

FIG. 1.1. *Thermal argon plasma inside an ICP torch.*

validity of this approximation and verify whether the obtained preliminary results make sense from both a qualitative and quantitative point of view.

2. Mathematical Model. The mathematical model is given by a simplified form of the equations of magneto-hydrodynamics [11, 10]. To a good approximation, the flow may be assumed to be under Local Thermodynamic Equilibrium (LTE) [10] and moreover mass fractions of elements can be fixed throughout the flow field in many situations [8]. We neglect buoyancy effects and time-average the equations over a period of the radio-frequency inductor current.

The governing equations then assume the following form [11]:

$$\nabla \cdot (\rho \mathbf{u}) = 0, \tag{2.1}$$

$$\nabla \cdot (\rho \mathbf{u} \otimes \mathbf{u}) + \nabla p = \nabla \cdot \tau + \langle \mathbf{F}_L \rangle, \tag{2.2}$$

$$\nabla \cdot (\rho \mathbf{u} H) = \nabla \cdot [(\lambda_{\text{tot}} + \lambda_{\text{react}}) \nabla T] + \langle P_J \rangle. \tag{2.3}$$

The flow is axisymmetric with swirl velocity component. For this reason, the equations have been implemented in cylindrical coordinates (z, r). For a detailed description, the reader is referred to [10]. We have introduced the following thermodynamic and transport properties: density $\rho = \rho(p, T)$, total enthalpy per unit mass $H = h + \|\mathbf{u}\|^2/2$ including internal enthalpy per unit mass $h = h(p, T)$, the total thermal conductivity coefficient $\lambda_{\text{tot}} = \lambda_{\text{tot}}(p, T)$, the reactive thermal conductivity coefficient $\lambda_{\text{react}} = \lambda_{\text{react}}(p, T)$ (see Ref. [8]) and the dynamic viscosity coefficient $\mu = \mu(p, T)$ appearing in the tensor of viscous stresses τ. Under LTE and for a given elemental composition, these quantities depend only on the pressure p and the temperature T. Further, $\mathbf{u} = (u, v)$ designates a mass-averaged flow velocity vector.

$\mathbf{F}_L$ represents the Lorentz force acting on the plasma and P_J stands for the Joule heating source term; the notation $\langle \cdot \rangle$ serves to indicate that the RMS average value is to be used for the latter two quantities. They have the following detailed expressions:

$$\langle P_J \rangle = \frac{\sigma \left(E_R^2 + E_I^2 \right)}{2} , \tag{2.4}$$

where E_R and E_I are real and imaginary part of an electric field, respectively and σ represents the electrical conductivity of the plasma. The time-averaged Lorentz force $\langle \mathbf{F}_L \rangle$ in cylindrical coordinates takes the form

$$\langle \mathbf{F}_L \rangle = \frac{\sigma}{4\pi f} \left(\left(\frac{E_R}{r} \frac{\partial_r E_I}{\partial z} - \frac{E_I}{r} \frac{\partial_r E_R}{\partial z} \right), \left(\frac{E_R}{r} \frac{\partial_r E_I}{\partial r} - \frac{E_I}{r} \frac{\partial_r E_R}{\partial r} \right), 0 \right)^{\mathrm{T}} , \tag{2.5}$$

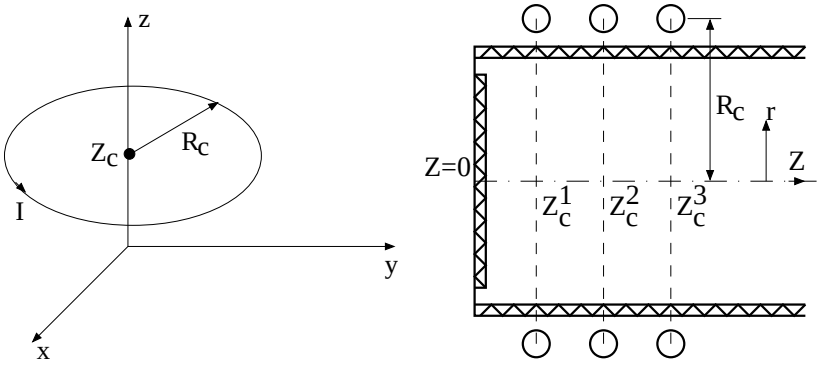

FIG. 3.1. *Schematic representation of the inductor coil surrounding a plasma torch. The current is assumed to flow at the innermost position of the inductor rings (infinitely thin current loops).*

where f is the operating frequency of the torch.

3. Electromagnetic Field. As a working assumption, we consider only the 'vacuum' electro-magnetic field E_V induced by the outer inductor in this preliminary study and disregard the contribution E_P induced by the plasma itself:

$$E = E_V + E_P \rightarrow E = E_V . \tag{3.1}$$

The coil surrounding the ICP torch (see Figure 1.1) is substituted by a series of (infinitely thin) current loops of radius R_c, carrying a current I (see Figure 3.1). The real and imaginary components of the 'vacuum' electric field intensity are as follows:

$$E_R = 0 , \tag{3.2}$$

$$E_I = -2\pi f A_R . \tag{3.3}$$

Only the azimuthal component of the vector potential is nonzero in our axisymmetric configuration (see, e. g., [4], [6]). It can be computed via the Biot-Savart law:

$$A_\theta(r,z) = A_R + jA_I = \frac{\mu_0 I}{2\pi}\sqrt{\frac{R_c}{r}} \sum_{i=1}^{\#\text{coils}} G(k_i) , \tag{3.4}$$

where $j = \sqrt{-1}$. Hence,

$$A_R = \frac{\mu_0 I}{2\pi}\sqrt{\frac{R_c}{r}} \sum_{i=1}^{\#\text{coils}} G(k_i) , \tag{3.5}$$

$$A_I = 0. \tag{3.6}$$

Here, #coils denotes number of cylindrical loops representing the inductor coil, μ_0 is the magnetic permeability of free space and

$$G(k_i) = \frac{(2-k_i^2)K_1(k_i) - 2K_2(k_i)}{k_i} , \tag{3.7}$$

$$k_i = \sqrt{\frac{4R_c r}{(R_c+r)^2 + (z-Z_c^i)^2}} , \tag{3.8}$$

where K_1 and K_2 are the complete elliptic integrals of the first and second kinds, respectively. For a numerical approximation of these integrals see, e. g., [9]. An illustration of magnetic field lines thus computed is shown in Figure 3.2.

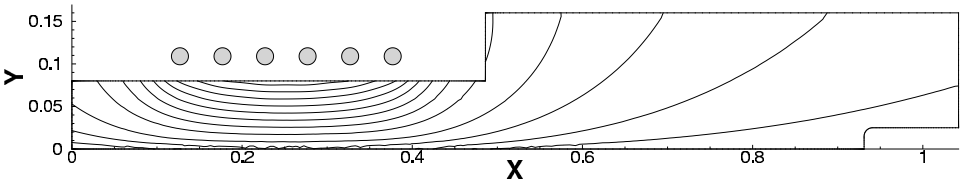

FIG. 3.2. *Illustration of 'vacuum' magnetic field lines for a six-turn coil around an ICP torch.*

4. Numerical Solution.

4.1. Pressure-Stabilized Flow Field Solver. Two variable sets are involved in the numerical solution of the equations (2.1) - (2.3). First, the solution is updated in primitive variables $P = (dp, u, v, T)^{\mathrm{T}}$, whereas the system (2.1) - (2.3) is expressed in conservative variables $U = (\rho, \rho u, \rho v, \rho E)^{\mathrm{T}}$:

$$\frac{U\left(P^{n+1}\right) - U\left(P^{n}\right)}{\Delta t} + \nabla \cdot \mathbf{F}\left(U\left(P^{n+1}\right)\right) = 0 \ , \tag{4.1}$$

where $\mathbf{F} = \left(F^C - F^V, G^C - G^V\right)$. Here, the superscript C denotes convective fluxes and V viscous fluxes. Symbol dp represents pressure variations. Relations for density ρ, total energy per unit mass E and total enthalpy per unit mass H come from statistical mechanics [10]. Eqs (4.1) are solved implicitly using a damped Newton method.

We use a pressure-stabilized finite-volume low-Mach number solver, such that the Jacobian of (4.1) is a regular matrix. The pressure-stabilized mass flux $\tilde{f}_M^{ed}$ normal to an edge ed (see Figure 4.1) is given by

$$\tilde{f}_M^{ed} = (\rho u_{\mathbf{n}})_{ed} - \frac{\Lambda}{\beta}\left(dp_{ed}^r - dp_{ed}^l\right) \ , \tag{4.2}$$

where $u_{\mathbf{n}} = \mathbf{u} \cdot \mathbf{n}_{ed}$, $\mathbf{n}_{ed} = \left(n_1^{ed}, n_2^{ed}\right)$ is the normal vector to the edge ed and

$$\Lambda = \frac{1}{1 + Re_{|ed|}^{-1}} \tag{4.3}$$

is a factor scaling the pressure dissipation with the local cell Reynolds number

$$Re_{|ed|}^{-1} = \frac{\mu}{\rho\beta|ed|}. \tag{4.4}$$

Here, β stands for an estimated global flow speed. Then, the stabilized convective flux vector $\tilde{F}_{ed}^c$ on the edge ed including upwind stabilization reads

$$\tilde{F}_{ed}^c = \begin{bmatrix} \tilde{f}_M^{ed} \\ (\rho u_{\mathbf{n}})_{ed} u_{ed} - 0.5|(\rho u_{\mathbf{n}})_{ed}|\left(u_{ed}^r - u_{ed}^l\right) + dp_{ed}\, n_1^{ed} \\ (\rho u_{\mathbf{n}})_{ed} v_{ed} - 0.5|(\rho u_{\mathbf{n}})_{ed}|\left(v_{ed}^r - v_{ed}^l\right) + dp_{ed}\, n_2^{ed} \\ \tilde{f}_M^{ed} h_{ed} - 0.5|(\rho u_{\mathbf{n}})_{ed}|\left(h_{ed}^r - h_{ed}^l\right) \end{bmatrix} . \tag{4.5}$$

If symbol var represents an arbitrary variable, then $var_{ed} = \left(var_{ed}^r + var_{ed}^l\right)/2$ and var_{ed}^r, resp. var_{ed}^l is a value of the variable var considered at the edge ed and coming from the finite volume cell Ω_r, resp. Ω_l. All simulations presented herein were run using a first-order upwind method as a first approach. Viscous fluxes were discretized in the standard finite-volume manner, using dual cells to evaluate derivatives on cell edges [10].

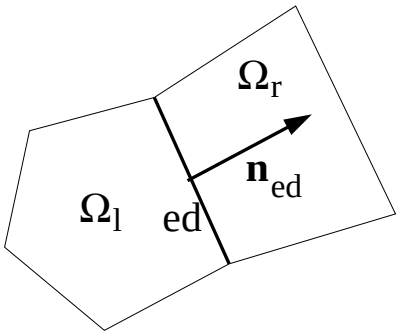

FIG. 4.1. *Computational stencil used to evaluate convective fluxes.*

4.2. Joule Heating Source Term. The power P_t dissipated into the plasma is given by the formula

$$P_t = \int_{V_T} \frac{\sigma \left(E_R^2 + E_I^2\right)}{2} \, dV \,, \tag{4.6}$$

where E_R and E_I are given by (3.2) and (3.3), respectively. The symbol V_T denotes the volume of the torch. This power is proportional to the square of the electric current running in the induction coils (see Eq. 3.4): $P_t \propto I^2$. The desired operating power P_0 can be expressed as

$$P_0 = \int_{V_T} \frac{\sigma \left((\gamma_c E_R)^2 + (\gamma_c E_I)^2\right)}{2} \, dV \propto (\gamma_c I)^2 \,, \tag{4.7}$$

where γ_c is a scaling coefficient. It is determined as follows

$$\gamma_c^2 = \frac{P_0}{P_t} \,. \tag{4.8}$$

This coefficient is used for rescaling the electric current I and thereby the electric field intensity, in order to have the desired power level P_0 at any iteration of the Newton method. Therefore, the Joule heating source term can be expressed as follows:

$$\langle P_J \rangle = \gamma_c^2 \frac{\sigma \left(E_R^2 + E_I^2\right)}{2} \,. \tag{4.9}$$

The relation (4.6), discretized in a finite volume manner, can be written in the form

$$P_t = \sum_{i=1}^{\#\text{cells}} \left\{ \frac{\sigma \left(E_R^2 + E_I^2\right)}{2} \right\}_i V_i \, 2 \, \pi \, r_i \,, \tag{4.10}$$

where V_i is the area of the i-th cell and r_i denotes the radius of the i-th cell centroid.

5. Numerical Results. We now present preliminary results for ICPs in the von Karman Institute's (VKI) 'plasmatron' windtunnel [1]. These results were obtained using an object-oriented CFD platform developed at VKI and extended for ICP features [5]. The Lorentz force is known to be negligible at the considered pressure levels [11] and has therefore not been implemented. Furthermore, as said (Eq. 3.1), the

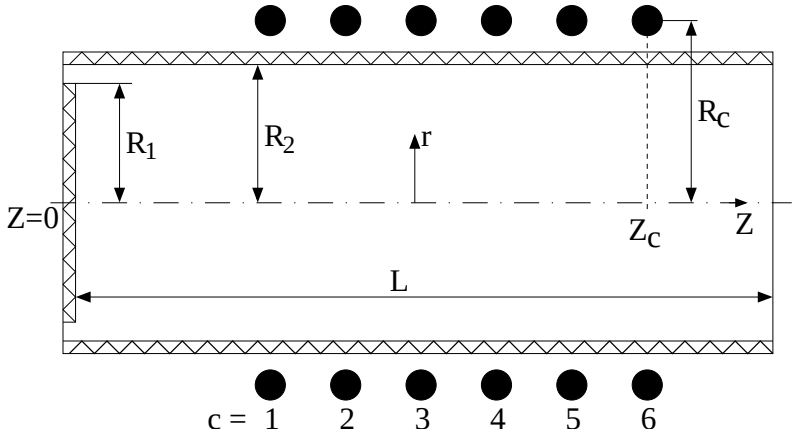

FIG. 5.1. *Plasmatron torch geometry used for our preliminary simulations.*

plasma-induced electric field intensity part E_P is set to zero. To assess the relative importance of the plasma-induced part of the electric field intensity in ICP flows, we write the induction equation that couples E_V and E_P in dimensionless form:

$$\frac{1}{\tilde{r}}\frac{\partial}{\partial\tilde{r}}\left(\tilde{r}\frac{\partial\tilde{E}_P}{\partial\tilde{r}}\right)-\frac{1}{\tilde{r}^2}\tilde{E}_P-jN_1\tilde{\sigma}\left(\tilde{E}_P+\tilde{E}_V\right)=0\,. \tag{5.1}$$

Here $\tilde{r}=r/R_\delta$, $\tilde{\sigma}=\sigma/\sigma_1$, $\tilde{E}_V=E_V/E_1$, $\tilde{E}_P=E_P/E_1$ and $E_1=2\pi\mu_0 fI$, where R_δ stands for the skin layer ($\approx$ thermal boundary layer) thickness, I is the amplitude of the electric current through the inductor rings and σ_1 represents an estimate of the plasma electrical conductivity. One dimensionless number has appeared as a result of the non-dimensionalization procedure:

$$N_1=2\pi\mu_0\sigma_1 fR_\delta^2\,. \tag{5.2}$$

This number is called 'induction number' and it characterizes the electromagnetic coupling between the coil and plasma. From equation (5.1), it is seen that it should be of order 1 or greater to achieve good inductive coupling.

Simulations are performed for the geometry (inspired by the VKI 'plasmatron' torch) shown on Figure 5.1, with dimensions

$$\begin{aligned} R_1 &= 0.075 \text{ m}\,,\\ R_2 &= 0.08 \text{ m}\,,\\ L &= 0.486 \text{ m}. \end{aligned}$$

The radii R_c and axial positions Z_c of the inductor rings are summarized in Table 5.1. If it is considered that $R_\delta \approx R/3 \approx 0.3$ m, then for the used values of $f = 0.37$ MHz, $\mu_0 = 4\pi\,10^{-7}$ kg m C^{-2} and $\sigma_1 \approx 3000$ S m^{-1} (for $T = 10000$ K) the induction number reaches the value $N_1 \approx 21$. We must therefore conclude that the electromagnetic coupling between E_V and E_P has a non-negligible effect on numerical results and that our decision to neglect E_P can only be a working assumption.

We consider Argon as a working gas (species: Ar, Ar^+, e^-). The operating parameters of the torch are: torch operating frequency $f = 0.37$ MHz, operating plasmatron torch power $P_0 = 10$ kW, mass flow rate at the inlet of the torch $Q = 8$ g s^{-1}, temperature imposed on the isothermal wall $T_w = 350$ K. A quadrilateral

Coil	R_c [m]	Z_c [m]
1	0.109	0.127
2	0.109	0.177
3	0.109	0.227
4	0.109	0.277
5	0.109	0.327
6	0.109	0.377

TABLE 5.1
Inductor rings radia and positions.

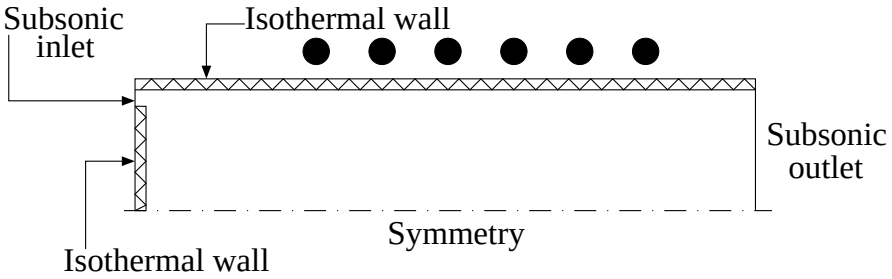

FIG. 5.2. *Boundary conditions of the computational domain (isothermal inlet wall).*

structured mesh of $116 \times 88 = 10208$ cells is used. The applied boundary conditions are given in Figure 5.2. The torch walls are treated as isothermal walls. Symmetry condition is imposed on the torch axis. Since the flow speed is subsonic, subsonic inlet and subsonic outlet boundary conditions are used.

Figure 5.3 shows the computed streamline pattern. The well-known clockwise vortex that stabilizes the plasma flame is correctly obtained. The frontiers of an overlapping domain-decompositioning (used for parallel computations on four processors) are also shown. Figure 5.4 shows computed temperature isolines. In spite of the drastic approximation made, quantatively correct peak temperatures $\approx 10\ 000$ K are reached in the inductor zone. A detailed comparison of presented numerical results with results considering both the Lorentz force and coupling of E_V with E_P is made in [5]. Finally, the good convergence achieved is evidence of the robustness of the proposed numerical techniques. Figure 5.5 presents the decadic logarithm of the L_2 norm of the temperature equation steady reziduum, which serves as the simulation stopping criteria, with respect to iterations of the Newton method.

6. Conclusions. The presented results show that, as a useful working assumption for developing numerical models of ICP flows, the plasma-induced electro-magnetic field may be neglected. Although our analysis showed that this approximation is not valid for most ICP torches, the obtained results nevertheless show correct physical trends and orders of magnitude. From a purely numerical point of view, the suggested numerical techniques have also been shown to yield a robust solution algorithm.

The logical next step in this research will be to include the plasma-induced electric field into the simulations.

Acknowledgment. This work has partly been supported by the Research Plan of the Ministry of Education of the Czech Republic No 6840770010.

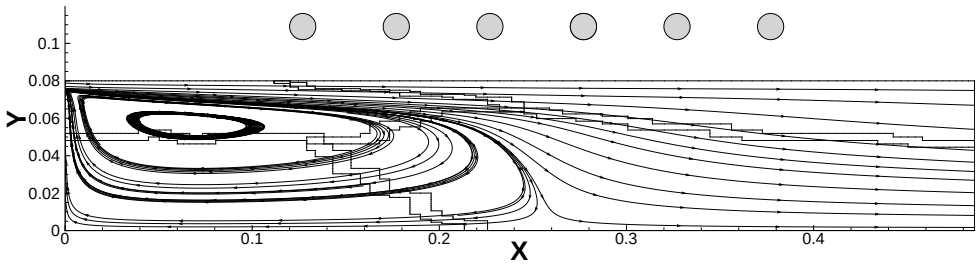

FIG. 5.3. *Streamline patterns.*

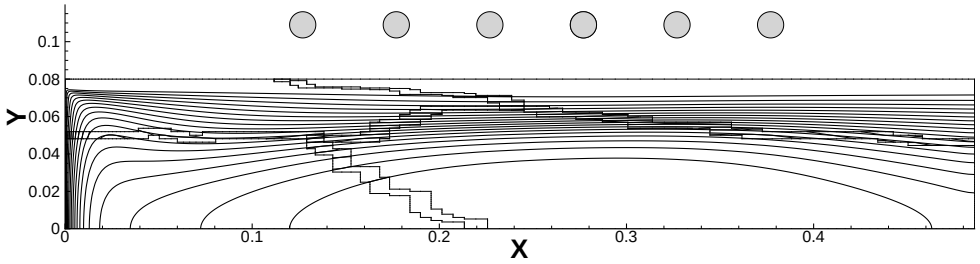

FIG. 5.4. *Temperature isolines.*

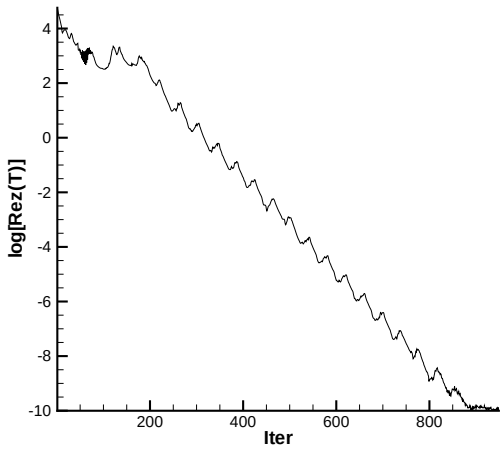

FIG. 5.5. *Convergence history demonstrating the robustness of the code.*

REFERENCES

[1] B. BOTTIN, M. CARBONARO, O. CHAZOT, G. DEGREZ, D. VANDEN ABEELE, P. BARBANTE, S. PARIS, V. VAN DER HAEGEN, TH. MAGIN, AND M. PLAYEZ, *A Decade of Aerothermal Plasma Research at the von Karman Institute*, Contributions to Plasma Physics **44** no. 5-6 (2004), 472–477.

[2] M. I. BOULOS, *Flow and Temperature Fields in the Fire-Ball of an Inductively Coupled Plasma*, IEEE Transactions on Plasma Science **PS-4**, no. 1 (1976), 28–39.

[3] M. I. Boulos, *The Inductively Coupled Radio Frequency Plasma*, Pure and Applied Chemistry, **57**, no. 9 (1985), 1321–1352.
[4] X. Chen, and E. Pfender, *Modeling of RF Plasma Torch with a Metallic Tube Inserted for Reactant Injection*, Plasma Chemistry and Plasma Processing **11**, no. 1 (1991), 103–128.
[5] R. Honzátko, H. Deconinck, D. Vanden-Abeele, A. Lani, M. Panesi, and T. Quintino, *Implementation of a Finite-Volume Inductively Coupled Plasma Model into the Object-Oriented Solver COOLFluiD*, Project Report 2006-16, VKI, June 2006.
[6] J. Mostaghimi, and M. I. Boulos, *Two-Dimensional Electromagnetic Field Effects in Induction Plasma Modelling*, Plasma Chemistry and Plasma Processing **9**, no. 1 (1989), 25–44.
[7] T. B. Reed, *Induction-Coupled Plasma Torch*, Journal of Applied Physics **32**, no. 5 (1961), 821–824.
[8] P. Rini, D. Vanden-Abeele, and G. Degrez, *Elemental Demixing in Inductively Coupled Air Plasma Torches at High Pressures*, Journal of Thermophysics and Heat Transfer, to appear, 2006.
[9] P. Silvester, *Modern Electromagnetic Fields*. Prentice Hall, New Jersey (1968).
[10] D. Vanden-Abeele, *An Efficient Computational Model for Inductively Coupled Air Plasma Flows under Thermal and Chemical Non-Equilibrium*, Phd thesis, VKI / Katholieke Universiteit Leuven, November 2000.
[11] D. Vanden-Abeele and G. Degrez, *Similarity Analysis for the High-Pressure Inductively Coupled Plasma Source*, Plasma Sources Science and Technology **13** (2004), 680–690.